Study of the data analysis process of the neutron wall with simulation [*]

LIU Long-Xiang(刘龙祥)[1,2,3]   SUN Zhi-Yu(孙志宇)[1;1)]   XIAO Guo-Qing(肖国青)[1]

CHEN Xi-Meng(陈熙萌)[2]   YU Yu-Hong(余玉洪)[1]   ZHANG Xue-Heng(章学恒)[1]

WANG Shi-Tao(王世陶)[1]   TANG Shu-Wen(唐述文)[1]   ZHOU Yong(周勇)[1,2,3]   YAN Duo(闫铎)[1,3]

[1] Institute of Modern Physics, Chinese Academy of Sciences, Lanzhou 730000, China
[2] School of Nuclear Science and Technology, Lanzhou University, Lanzhou 730000, China
[3] University of Chinese Academy of Sciences, Beijing 100049, China

Abstract: We study the response function of the neutron wall for 300 MeV neutrons with GEANT4 simulations. The methods to find the correct neutron incident position and time are discussed, and the neutron emission angle and energy are reconstructed and compared with the simulation.

Key words: neutron wall, GEANT4 simulation, parallel computation

PACS: 29.40.Gx, 29.40.Mc, 29.85.Fj   **DOI:** 10.1088/1674-1137/37/9/096201

1 Introduction

The successful construction and commissioning of the HIRFL-CSR at the Institute of Modern Physics, Chinese Academy of Sciences, offer us a good opportunity to study the nuclear reactions and properties with heavy ion beams of several hundred MeV in China. Some new detectors are built for the purpose, and the neutron wall is one of them.

The neutron wall, which is located at the external target experimental hall of CSRm, has been built to measure the neutrons from near-relativistic heavy-ion collisions by the time of flight (TOF) method. Fig. 1 shows the sketched drawing of the detector, and a detailed description can be found in Ref. [1].

A neutron with several hundred MeV energy may generate many high-energy electrons, positrons or photons in the neutron wall, an electromagnetic shower begins when one of which enters the material of the detector. The electro-magnetic showers in the neutron wall will fire many detector modules within a large range nearly at the same time. Therefore, how to find the original points of incident neutrons is a key problem for the data analysis of all the large neutron detector arrays working in this energy region like the neutron wall, and the Monte-Carlo simulation will be a good way to study the solutions.

In this paper we will show some results for the neutron wall data analysis studied with the GEANT4 simulations.
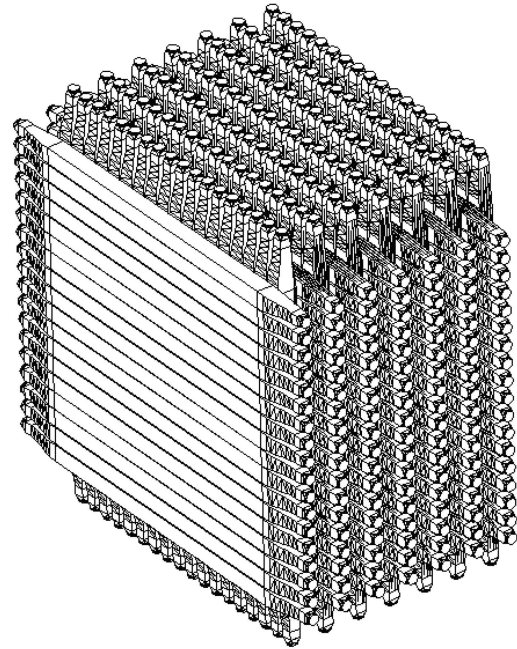
Fig. 1.   Sketch of the neutron wall.

2 The simulation method

Geant4 is an ideal framework for modeling the scintillator detectors and its associated light guides. This is due to its unique capacity of commencing the simulation with the propagation of a charged particle and completing it with the detection of the ensuing photons

on light-sensitive areas, all within the same event loop.

In the simulation, the energy of a neutron is set as 300 MeV, which is typical for the experiments that will be performed with use of the neutron wall. The neutrons are emitted from the target position which is 13.325 m upstream of the neutron wall, and they have a homogeneous polar angle distribution between 0 to 3.09°. Neutron source θ/ϕ distribution is shown in Fig. 2.
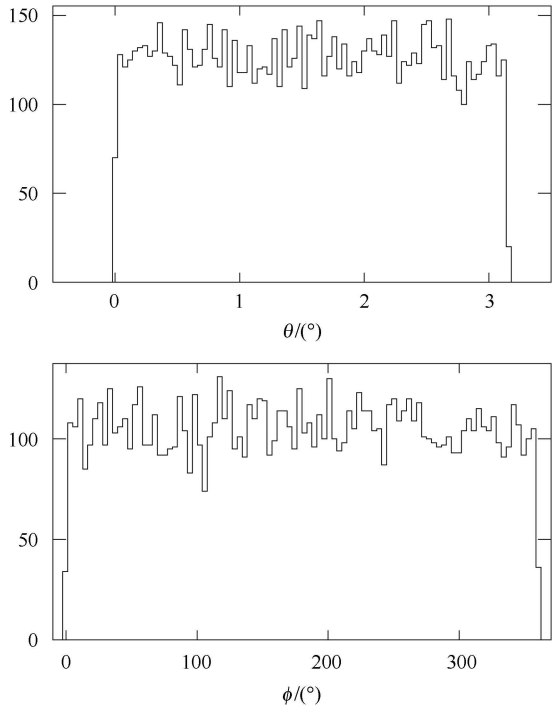
Fig. 2.   Neutron source θ/ϕ distribution.

The plastic scintillator BC408 is used in the neutron wall, and its relevant properties are listed in Table 1. When a neutron hits the detector, secondary charged particles will be produced and they will deposit energy in the scintillator. One photon will be produced for an average of 100 eV energy deposition, and the produced photons have isotropic angular distribution.

Table 1.   Parameters of BC408.

density/(g/cm^3)	1.032
refraction index	1.58
rise time/ns	0.9
decay time/ns	2.1
atten. length/cm	380

The processes considered in the simulation for visible light include refraction and reflection at medium boundaries, bulk absorption and Rayleigh scattering. The optical properties of the mediums, which are very important to the implementation of these processes and can be expressed as a function of the photon's wavelength [2], are

stored as entries in a specified table linked to the materials in question.

The cosmic ray is used to get the effective velocity of light in the detector modules, and this process is also simulated. The particle used in simulation is $\mu-$ with 4 GeV energy [3], and its position and direction of emission are the same as those of the neutrons mentioned above.

The effective velocity of light in a module is calculated by Eq. (1) as

$$v_{\text{eff}} = \frac{l}{(t_l + t_r) - 2 \times t_s}, \qquad (1)$$

where l denotes the length of the module, t_l and t_r represent the time information obtained by the PMTs at the left and right ends of the module, respectively, and t_s is the time for the original interaction, which, of course, is not accessible to a measurement. Photons produced in a module are collected by the light guides on both ends and guided to the PMTs. The amplitude of the output signal is proportional to the number of photons collected in the cathode of the PMTs. Because the leading-edge discriminator is used to get the time information in the measurement, the calculated effective velocity will be influenced by the threshold of the discriminator, which corresponds to a certain number of photons collected. Some simulations are made in terms of different number of photons, and the calculated effective velocity of light is shown in Table 2. The values of the second group are similar to the ones obtained from the experiment 16.0 cm/ns and 15.4 cm/ns, respectively, which are taken from Ref. [4]. Therefore, we regard the arriving time of the 43th photon as the time information obtained from the experiment.

Table 2.   The effective velocity of light. v_{sci} is the effective velocity of light for the modules of the front two layers and v_{abs} for the other layers.

photon No.	v_{sci}	v_{abs}
40th	16.13	15.53
43th	15.97	15.42
45th	15.90	15.32

Under the help of TOP-C [5] and Marshalgen [6], ParGEANT4 is set up. With this new ParGEANT4 simulation program, we get a nearly linear boost up in the computing time, for example 3.72 times faster with 4 nodes than one node.

3   Results and discussion

For each incident high-energy neutron, a "shower" will occur in the neutron wall and many modules will be fired during this process. Fig. 3(a) shows the distributions of fired modules by a 300 MeV neutron with different thresholds of the discriminator.
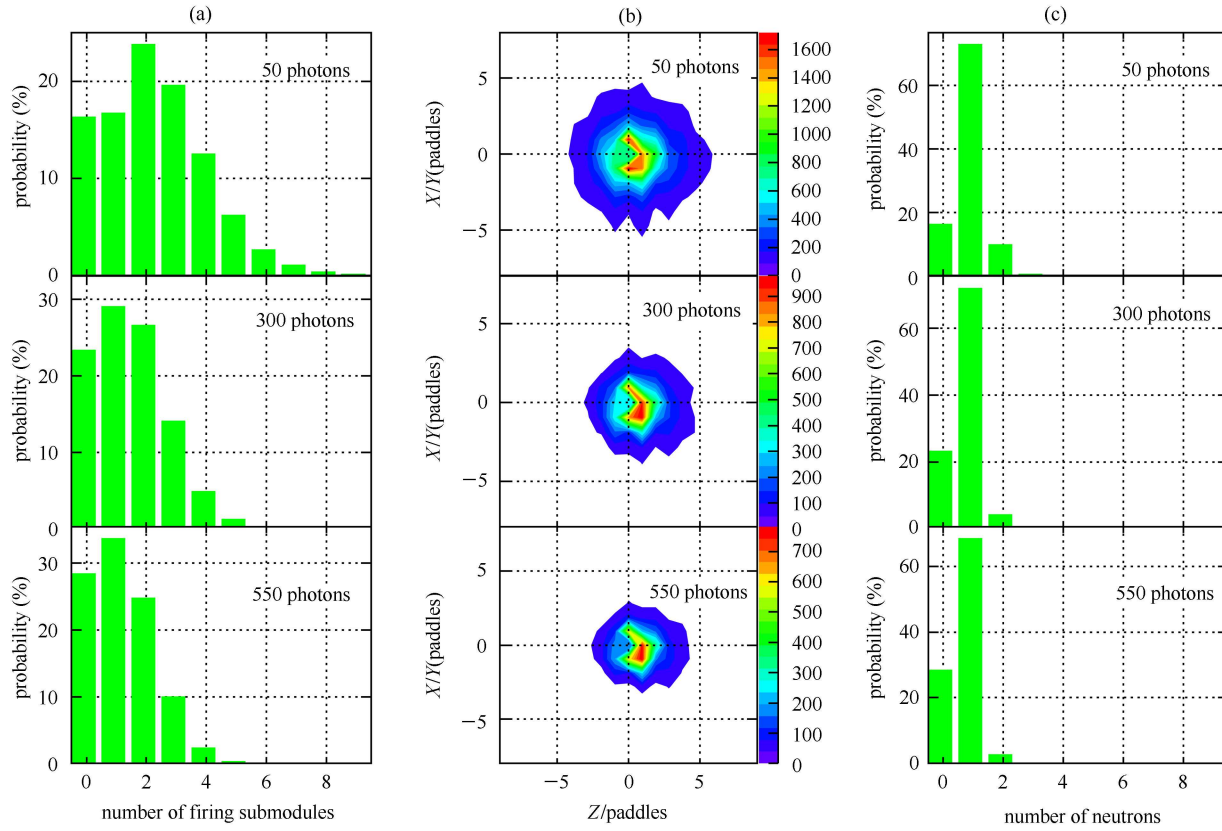
Fig. 3.   (color online) The simulated fired paddles distribution of neutron wall to 300 MeV neutrons for three different thresholds. Column (a): the average probability of the different number of fired submodules per incident neutron; Column (b): the relative paddle number in transverse direction between the submodule fired first and the submodules fired subsequently vs. that in longitudinal direction between them; Column (c): the average probability that an event with one neutron is misinterpreted as an event with a different number of neutrons.

For each module, the hit information (position and time) can be obtained with Eq. (2) and Eq. (3), respectively.

$$x = \frac{(t_l - t_r)}{2} \times v_{eff}, \qquad (2)$$

$$t = \frac{t_l + t_r - l/v_{eff}}{2}. \qquad (3)$$

We regard the one with the earliest hit time as the start point of the "shower", and the position distributions of the hits, which are centered at the corresponding start points, with different thresholds are shown in Fig. 3(b).

Figure 4 shows the distance distribution of the start point to the other hits with the threshold corresponding to 50 photons. All the hits in a zone, which is marked in Fig. 4, are regarded as contributions of the same neutron, and the zone we defined is 3 paddles upstream and 6 paddles downstream in longitudinal direction and 4 paddles in transverse direction around the start point. It is a little larger than the ones of LAND [7], whose "shower" volume is 29 cm in radius and 50 cm in depth around the first hit.
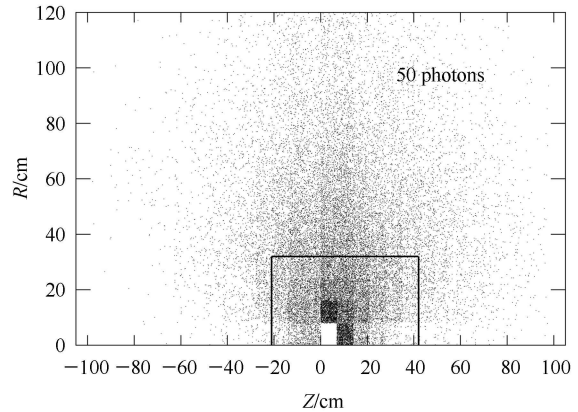
Fig. 4.   The distance distribution between the submodule fired first and submodules fired subsequently ($R = \sqrt{X^2 + Y^2}$).

For the hits which remain, the same procedure will be reiterated. Because one neutron may interact with the detectors more than once in distant points, these points may be regarded as separated clusters by the procedure. To take this into account, we add a simple "long-range

correlation" to search for distant clusters correlated in time and space. With this correlation, we estimate the velocity of incident neutron for all the clusters previously determined, and for the ones whose incident time fulfills the relation Eq. (4), they will be regarded as one.

$$\left|\Delta t - \frac{d}{v}\right| \leqslant 1\text{ns}, \tag{4}$$

here Δt is the time between the two hits, d is the distance between the two hits and v is the velocity of the incident neutron determined by the first hit.

Figure 3(c) shows the incident neutron multiplicity obtained with our analysis procedure. The results with different thresholds show that the efficiency for getting correct incident neutron information is not influenced much by the thresholds, and we can always get about 70%–80% accuracy. But for the possibility of misidentifying a neutron, it drops rapidly while the threshold is increased. Therefore, a higher threshold, such as 300 photons, is more suitable for the neutron wall detector in the future experiments.

Due to the limited resolutions in a real measurement,

we can only define a small cubic region for the original incident point through the geometry of the modules fired instead of the precise position in the simulations. We define the center of this cubic volume as the incident point, and apply the same procedure to the simulation data analysis. So, considering the size of the modules, we get an intrinsic uncertainty of $\Delta X = \pm 4$ cm, $\Delta Y = \pm 4$ cm and $\Delta Z = \pm 3.5$ (± 4 cm if located in the first two layers).

ΔS is defined as the distance between the start point extracted with the procedure mentioned above and the exact one obtained from the simulation. Fig. 5(a) shows the distribution of ΔS with three different thresholds, and we can see that the most probable value of ΔS is around 4 cm, which reflects the cross section of the modules.

If the original incident point is defined, we can calculate the kinetic energy of the incident neutron from L and t by the time of flight method. Here $L = (X^2 + Y^2 + Z^2)^{1/2}$ is the length of the flight path, and t is the time obtained by the mean-timing from both ends of the corresponding module with Eq. (3).
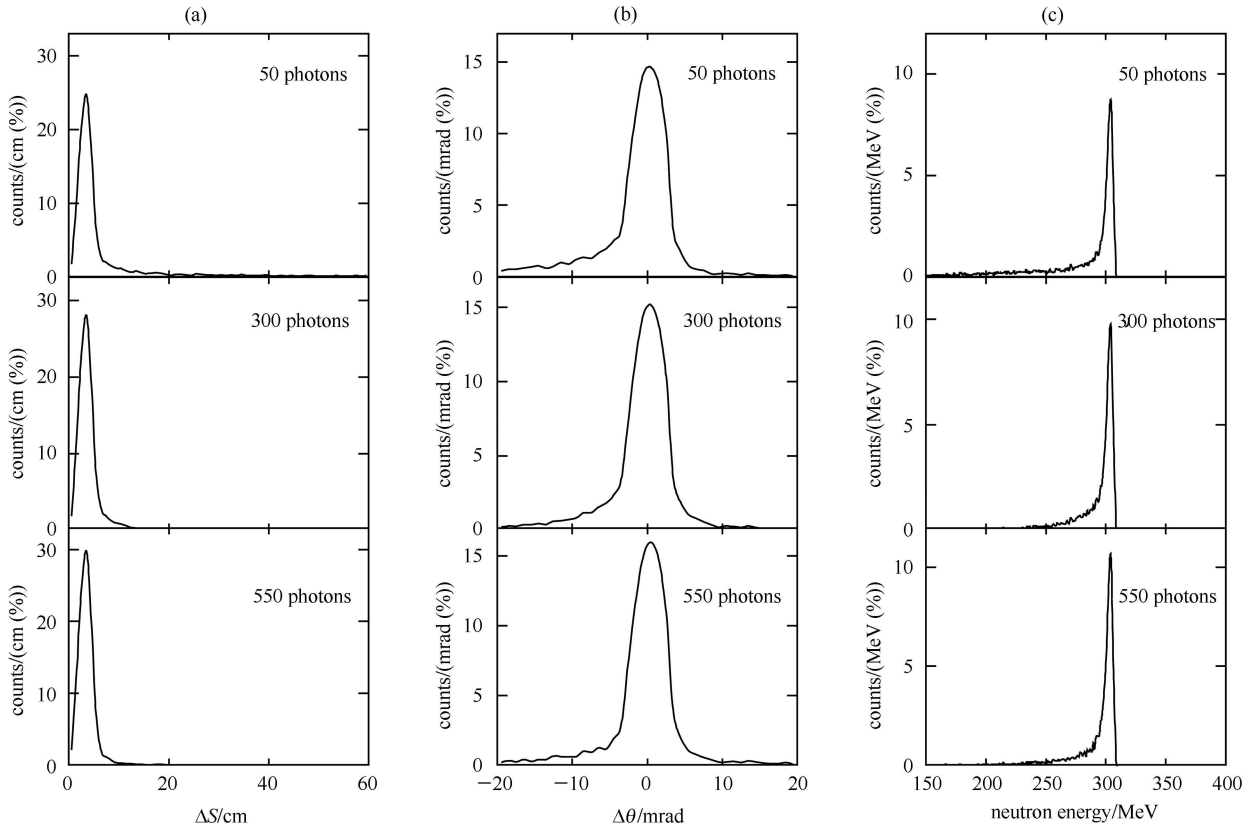
Fig. 5.   The simulated response function of the neutron wall to 300 MeV neutrons of three different thresholds. Column (a): deviation, ΔS, of the position of the first interaction to that of the first visible energy production; Column (b): change of the neutron angle due to ΔS; Column (c): kinetic energy of neutrons as determined from time-of-flight and the measured position of the first visible energy production.

After obtaining this start point, we can reconstruct the emission angle of the neutrons from the target, and Fig. 5(b) shows our results compared with the precise ones in the simulation. This angular uncertainty, which has a width of about 2 mrad and is nearly independent of the threshold, mainly comes from the uncertainty of the start point position, and it will cause an error on the length of the flight path and influence the neutron energy calculated from the time of flight.

Figure 5(c) shows the reconstructed neutron energy for the 300 MeV neutrons, and we can see that the neutron energy can be well reproduced by the procedure mentioned above. The width of the obtained energy distribution is about 2.5 MeV (σ), and it is nearly independent of the thresholds.

This energy uncertainty comes from two aspects. One is the time resolution of the read-out devices, and another is the uncertainty of the flight path, which is mainly due to the incident angular uncertainty. In our analysis, the first one contributes about 2.1 MeV to the σ, and the second part contributes about 1.7 MeV. Because the method we used to get the time is similar to the leading-edge discriminator in the measurement, the first part can be reduced greatly by using the pulse amplitude correc-

tion, and the contributions from the uncertainty of the flight path will play a more important role in the real experiments.

4 Summary

The response of the neutron wall for 300 MeV neutrons is studied with the GEANT4 simulation, and we developed the parallel programs to reduce the CPU time needed. Our results show that the high-energy neutrons may fire many detector modules within a large volume, which makes the data analysis very complicated. We find a way to obtain the right position and time of the original incident point with high enough accuracy and efficiency, and the energy and emission angle of the neutrons are reconstructed. The uncertainty of the emission angle is about 2 mrad, which is mainly due to the size of each module. For the neutron energy, a σ of about 2.5 MeV is obtained, and the contributions from the time resolution may be reduced by using amplitude-timing correction. Because both the energy and angle resolution drop a little while the threshold of the PMTs is increased, it's better to use a higher threshold in the experiment.

References

1 XU Hua-Gen, XU Hu-Shan, LI Wen-Fei et al. HEP & NP, 2006, **30**: 57 (in Chinese)
2 Agostinelli S, Allsion J, Amako K et al. Nucl. Instrum. Methods A, 2003, **506**: 250
3 Groom D E, Aguilar-Benitez M, Amsler C et al. Eur. Phys. J. C, 2000, **15**: 151
4 YU Yu-Hong. Development and Construction of Fast Plastic Scintillator Detector Array for External Target Experiment at CSRm(Ph.D.Thesis). Lanzhou: Institute of Modern Physics, CAS, 2009 (in Chinese)
5 http://www.ccs.neu.edu/home/gene/topc.html
6 http://www.ccs.neu.edu/home/gene/marshalgen.html
7 Zinser M, Humbert F, Nilsson T et al. Nucl. Phys. A, 1997, **619**: 151